IEEE Access
Multidisciplinary | Rapid Review | Open Access Journal

Received December 23, 2019, accepted January 7, 2020, date of publication January 20, 2020, date of current version January 29, 2020.

Digital Object Identifier 10.1109/ACCESS.2020.2967818

State Estimation of Continuous-Time Linear Fractional-Order Systems Disturbed by Correlated Colored Noises via Tustin Generating Function

XIAOMIN HUANG[1], ZHE GAO[1,2,3], CHAO YANG[1], AND FANGHUI LIU[1]

[1]School of Mathematics, Liaoning University, Shenyang 110036, China
[2]College of Light Industry, Liaoning University, Shenyang 110036, China
[3]Department of Control Science and Engineering, Jilin University, Changchun 130025, China

Corresponding author: Zhe Gao (gaozhe@lnu.edu.cn)

This work was supported in part by the Liaoning Revitalization Talents Program under Grant XLYC1807229, in part by the Natural Science Foundation of Liaoning Province, China, under Grant 20180520009, in part by the China Postdoctoral Science Foundation Funded Project under Grant 2019M651206, and in part by the Scientific Research Foundation of Liaoning University under Grant LDGY201920.

ABSTRACT This paper proposes Kalman filters to investigate the state estimation of continuous-time linear fractional-order systems disturbed by correlated colored noises. A difference equation is obtained by discretizing the fractional-order differential equation via Tustin generating function. Besides, an augmented vector is determined by the state vector and the colored noise vector to deal with the problems on the colored process noise or the colored measurement noise with fractional-orders. In fact, a more accurate state estimation can be achieved using the discretization method via Tustin generation function for the investigated fractional-order systems, compared with Grünwald-Letnikov difference. Finally, two illustrative examples are provided to validate the effectiveness of the proposed algorithms in this paper.

INDEX TERMS State estimation, fractional-order Kalman filters, Tustin generating function, colored noises, correlated noises.

I. INTRODUCTION

With the development of modern science, a lot of experts have pointed out that fractional-order systems (FOSs) can better describe the behaviors of real-world systems such as systems with viscoelastic [1] and anomalous diffusive characteristics [2]. The introduction of fractional-order calculus makes the controller design more flexible such as the fractional-order sliding mode controllers [3], the fractional-order iterative learning controllers [4] and the fractional-order PID controllers [5]. Meanwhile, a satisfactory control performance of closed loop systems is achieved with the memory property of fractional-order operations. Therefore, the modeling and control of FOSs [6] have attracted much attention recently.

For integer-order systems, many methods of state estimation for linear and nonlinear systems have been reported such as the linear filters [7], the fuzzy observers [8], the particle filters [9], the Kalman filters (KFs) [10], the cubature Kalman filters (CKFs) [11], the unscented Kalman filters [12], the optimal and suboptimal algorithms [13]–[15]. The state information of FOSs is more complicated to estimate compared with integer-order systems, due to the memory property of fractional-order calculus. But KF can still be applied to FOSs to achieve the robust state estimation. The fractional-order Kalman filters (FOKFs) were proposed in [16] to estimate the state information for FOSs involving noise. The extended Kalman filter (EKF) was offered in [17] to estimate the state information of nonlinear FOSs, and this method gained a better estimation performance. For discrete-time linear and nonlinear FOSs, the FOKFs were proposed in [18] to achieve state estimation. For discrete-time nonlinear FOSs, an adaptive three-stage EKF was given in [19] to improve the accuracy of state estimation

All of the above discussed noises in FOSs are white Gaussian noises, but it is necessary to explore the non-white and non-Gaussian noises in real-world systems. The FOKFs were presented in [20] and [21] for linear and nonlinear FOSs with Lévy noises in the measurement signals to estimate

The associate editor coordinating the review of this manuscript and approving it for publication was Pietro Savazzi.

effectively state information, respectively. The FOKFs were studied in [22] to estimate the state for linear FOSs with fractional-order colored measurement noises. To deal with the correlated noises, the FOKFs were discussed in [16] to make lower the estimation error caused by the correlated noises. The CKFs via Grünwald-Letnikov difference (GLD) were derived in [23] to estimate effectively state and parameters of continuous-time nonlinear FOSs involving the uncorrelated and correlated noises. For continuous-time nonlinear FOSs, the EKFs were discussed in [24] to deal with the correlated fractional-order colored noises. Besides, the KF for nonlinear FOSs with correlated colored measurement noises was given in [25] by converting the discussed FOS to a FOS with white Gaussian noises.

In fact, the discretization is an important step to transform the differential equation into a difference equation for a continuous-time FOS. In [26] and [27], some related original discretization methods such as the Euler transform, the bilinear transform, the generalized bilinear transform, Z-S transform were put forward. In [24], the discretized methods via GLD and Tustin generating function (TGF) were used to obtain the state and parameter information. In [28], the fractional-order average derivative method for FOKFs was provided to estimate the state information of continuous-time linear FOSs with colored noises, improving the accuracy of state estimation.

It is a major issue in this paper that FOKFs based on TGF are designed to estimate the state information of continuous-time linear FOSs with correlated colored noises. Then, the main achievements in this paper are summarized: 1. TGF is adopted to discretize the fractional-order differential equation with respect to the state and noises to obtain the corresponding difference equation. 2. The colored process noise or colored measurement noise with fractional-orders are dealt with using the augmented vector method determined by the state vector and the colored noise. 3. FOKFs based on TGF are presented to gain more accurate estimation of the state information, compared with GLD. 4. For different sampling periods, fractional-orders and the correlation matrices of noises, we draw the conclusions that the algorithms provided in this paper carry out the state estimation for the investigated FOS effectively, and the accuracy of state estimation via TGF is higher than GLD.

The rest of this paper is organized as follows. In Section II, some definitions of fractional-order operators are introduced. In Section III, the FOKF for the continuous-time linear FOS perturbed by the correlated fractional-order colored process noise and white Gaussian measurement noise is presented, and the case for the continuous-time linear FOS perturbed by the correlated white Gaussian process noise and fractional-order colored measurement noise is also discussed, similarly. Then, two examples are provided to validate the effectiveness of the proposed algorithms in Section IV. Finally, the whole paper is summarized in Section V.

II. PRELIMINARIES

For the investigated FOSs with correlated colored noises, the Caputo definition is adopted to study FOKFs because of the consistency of initial conditions of FOSs.

Definition 1: The GLD with α-order is provided by [29]

$$\Delta^{\alpha}x(\iota)=\frac{1}{T^{\alpha}}\sum_{\rho=0}^{+\infty}(-1)^{\rho}\binom{\alpha}{\rho}x(\iota-\rho), \tag{1}$$

where the sampling period is T, the α-order difference operation is Δ^{α}, and the factor $\binom{\alpha}{\rho}$ is represented by

$$\binom{\alpha}{\rho}=\begin{cases}1 & \rho=0\\ \dfrac{\alpha(\alpha-1)\ldots(\alpha-\rho+1)}{\rho!} & \rho>0.\end{cases}$$

Considering the following FOS

$$ {}_0^C D_{\tau}^{\alpha}x(\tau)=Ax(\tau)+Bu(\tau)+Gw(\tau), \tag{2}$$

$$ z(\tau)=Cx(\tau)+v(\tau), \tag{3}$$

where the α-order derivative is ${}_0^C D_{\tau}^{\alpha}$ from 0 to τ via Caputo definition [29], the fractional-order satisfies $\alpha\in(0,2)$, the state vector is $x(\tau)\in\mathbb{R}^n$, the input and measurement are $u(\tau)\in\mathbb{R}^p$ and $z(\tau)\in\mathbb{R}^q$, the process noise and measurement noise are $w(\tau)\in\mathbb{R}^m$ and $v(\tau)\in\mathbb{R}^q$ respectively, $A\in\mathbb{R}^{n\times n}$, $B\in\mathbb{R}^{n\times p}$, $G\in\mathbb{R}^{n\times m}$ and $C\in\mathbb{R}^{q\times n}$.

We denote $x(\iota)$, $u(\iota)$, $z(\iota)$, $v(\iota)$ and $w(\iota)$ for convenience as $x(\tau)$, $u(\tau)$, $z(\tau)$, $v(\tau)$ and $w(\tau)$ at $\tau=\iota T$ in this paper. For $\rho>\iota$, $x(\iota-\rho)=0$ in (1), the α-order derivative via the GLD is represented approximately by

$${}_0^C D_{\tau}^{\alpha}x(\iota)\approx\Delta^{\alpha}x(\iota)=\frac{1}{T^{\alpha}}\sum_{\rho=0}^{\iota}(-1)^{\rho}\binom{\alpha}{\rho}x(\iota-\rho).$$

Thus, we discretize the equation (2) as follows

$$x(\iota)=A_{\alpha}x(\iota-1)+B_{\alpha}u(\iota-1)+G_{\alpha}w(\iota-1)+\sum_{\rho=2}^{\iota}(-1)^{\rho+1}\Upsilon_{\rho}x(\iota-\rho), \tag{4}$$

where $A_{\alpha}=T^{\alpha}A+\alpha I$, $G_{\alpha}=T^{\alpha}G$, $B_{\alpha}=T^{\alpha}B$, and $\Upsilon_{\rho}=\binom{\alpha}{\rho}$.

The discretized method is very important to the realization of FOSs. To improve the accuracy of estimation for the state of the investigated FOSs, TGF [30] is adopted to transform the fractional-order derivative ${}_0^C D_{\tau}^{\alpha}x(\tau)$ into

$${}_0^C D_{\tau}^{\alpha}x(\tau)\approx(\frac{2}{T})^{\alpha}(\frac{1-p^{-1}}{1+p^{-1}})^{\alpha}x(\iota), \tag{5}$$

where $p^{-\rho}x(\iota)=x(\iota-\rho)$.

Accordingly, we discretize the state equation of the FOS as

$$(\frac{2}{T})^{\alpha}(\frac{1-p^{-1}}{1+p^{-1}})^{\alpha}x(\iota)=Ax(\iota)+Bu(\iota)+Gw(\iota). \tag{6}$$

Then, two kinds of FOKFs are studied based on TGF to solve the problem on correlated colored noises in the FOS defined by (2) and (3), respectively.

III. MAIN RESULTS

A. TREATMENT ON COLORED PROCESS NOISE PROBLEM

For this case, the sampling value $w(\iota)$ and the sampling value $v(\iota)$ are correlated. The noise $v(\iota)$ is white Gaussian noise with $E[v(\iota)] = \mathbf{0}$ and $E[v(\iota)v^T(\kappa)] = R\delta(\iota-\kappa)$, where $\delta(\iota-\kappa)$ is determined by $\delta(\iota-\kappa) = 0$ for $\iota \neq \kappa$ and $\delta(\iota-\kappa) = 1$ for $\iota = \kappa$. The process noise $w(\tau)$ is produced by

$$ {}_0^C D_\tau^\beta w(\tau) = Fw(\tau) + H\varepsilon(\tau), \tag{7} $$

where $\beta \in (0,2)$, $F \in \mathbb{R}^{m\times m}$, $H \in \mathbb{R}^{m\times r}$, the sampling value $\varepsilon(\iota) \in \mathbb{R}^r$ is the white Gaussian noise with $E[\varepsilon(\iota)] = \mathbf{0}$, $E[\varepsilon(\iota)\varepsilon^T(\kappa)] = Q\delta(\iota-\kappa)$, $E[\varepsilon(\iota)v^T(\kappa)] = \mathcal{W}\delta(\iota-\kappa) \neq \mathbf{0}$, $\mathbf{0}$ is the zero matrix of the appropriate dimension, and $E[\cdot]$ returns the mathematical expectation.

Furthermore, the process noise $w(\tau)$ based TGF is discretized as

$$ (\frac{2}{T})^\beta (\frac{1-p^{-1}}{1+p^{-1}})^\beta w(\iota) = Fw(\iota) + H\varepsilon(\iota). \tag{8} $$

The equations (6) and (8) via the generalized binomial theorem can be expanded by

$$ \begin{aligned} &(\frac{2}{T})^\alpha \sum_{\rho=0}^{\iota} (-1)^\rho \binom{\alpha}{\rho} x(\iota-\rho) \\ &\quad = \sum_{\rho=0}^{\iota} \binom{\alpha}{\rho} (Ax(\iota-\rho) + Bu(\iota-\rho) + Gw(\iota-\rho)), \end{aligned} \tag{9} $$

and

$$ \begin{aligned} &(\frac{2}{T})^\beta \sum_{\rho=0}^{\iota} (-1)^\rho \binom{\beta}{\rho} w(\iota-\rho) \\ &\quad = \sum_{\rho=0}^{\iota} \binom{\beta}{\rho} (Fw(\iota-\rho) + H\varepsilon(\iota-\rho)). \end{aligned} \tag{10} $$

Letting I be the identity matrix with the appropriate dimension, we choose T to make $(\frac{2}{T})^\alpha I - A$ and $(\frac{2}{T})^\beta I - F$ be invertible. Then, the equations (9) and (10) can be represented by

$$ x(\iota) = \sum_{\rho=1}^{\iota} \mathcal{A}_\rho x(\iota-\rho) + \sum_{\rho=0}^{\iota} \mathcal{B}_\rho u(\iota-\rho) + \sum_{\rho=0}^{\iota} \mathcal{G}_\rho w(\iota-\rho), \tag{11} $$

$$ w(\iota) = \sum_{\rho=1}^{\iota} \mathcal{F}_\rho x(\iota-\rho) + \sum_{\rho=0}^{\iota} \mathcal{H}_\rho \varepsilon(\iota-\rho), \tag{12} $$

where

$$ \begin{aligned} \mathcal{A}_\rho &= \left((\frac{2}{T})^\alpha I - A\right)^{-1} \binom{\alpha}{\rho} \left[(-1)^{\rho+1}(\frac{2}{T})^\alpha I + A\right], \\ \mathcal{B}_\rho &= \left((\frac{2}{T})^\alpha I - A\right)^{-1} \binom{\alpha}{\rho} B, \\ \mathcal{G}_\rho &= \left((\frac{2}{T})^\alpha I - A\right)^{-1} \binom{\alpha}{\rho} G, \\ \mathcal{F}_\rho &= \left((\frac{2}{T})^\beta I - F\right)^{-1} \binom{\beta}{\rho} \left[(-1)^{\rho+1}(\frac{2}{T})^\beta I + F\right], \\ \mathcal{H}_\rho &= \left((\frac{2}{T})^\beta I - F\right)^{-1} \binom{\beta}{\rho} H. \end{aligned} $$

To deal with the colored process noise $w(\iota)$, the augmented vector $\eta(\iota) = [x^T(\iota), w^T(\iota)]^T$ is defined, then the description of the augmented equation is yielded equivalently as

$$ \eta(\iota) = \sum_{\rho=1}^{\iota} \widetilde{\mathcal{A}}_\rho \eta(\iota-\rho) + \sum_{\rho=0}^{\iota} \widetilde{\mathcal{B}}_\rho u(\iota-\rho) + \sum_{\rho=0}^{\iota} \widetilde{\mathcal{H}}_\rho \varepsilon(\iota-\rho), \tag{13} $$

where $\widetilde{\mathcal{A}}_\rho = \begin{bmatrix} \mathcal{A}_\rho & \mathcal{G}_\rho + \mathcal{G}_0\mathcal{F}_\rho \\ \mathbf{0} & \mathcal{F}_\rho \end{bmatrix}$, $\widetilde{\mathcal{B}}_\rho = \begin{bmatrix} \mathcal{B}_\rho \\ \mathbf{0} \end{bmatrix}$ and $\widetilde{\mathcal{H}}_\rho = \begin{bmatrix} \mathcal{G}_0\mathcal{H}_\rho \\ \mathcal{H}_\rho \end{bmatrix}$.

From the equation (3), the output equation is represented by $z(\iota) = \widetilde{C}\eta(\iota) + v(\iota)$ with $\widetilde{C} = [C, \mathbf{0}]$.

The estimation and the prediction of $\eta(\iota)$ are denoted as $\widehat{\eta}(\iota|\iota) = E[\eta(\iota)|\sigma(\iota)]$ and $\widehat{\eta}(\iota|\iota-1) = E[\eta(\iota)|\mu(\iota)]$ respectively, where $\sigma(\iota)$ includes the information of $z(0), z(1), \ldots, z(\iota), u(0), u(1), \ldots, u(\iota)$ and $\mu(\iota)$ includes $z(0), z(1), \ldots, z(\iota-1), u(0), u(1), \ldots, u(\iota)$. Then, the prediction $\widehat{\eta}(\iota|\iota-1)$ is represented by

$$ \begin{aligned} \widehat{\eta}(\iota|\iota-1) &= E[(\sum_{\rho=1}^{\iota} \widetilde{\mathcal{A}}_\rho \eta(\iota-\rho) + \sum_{\rho=0}^{\iota} \widetilde{\mathcal{B}}_\rho u(\iota-\rho) \\ &\quad + \sum_{\rho=0}^{\iota} \widetilde{\mathcal{H}}_\rho \varepsilon(\iota-\rho))|\mu(\iota)] \\ &= E[\sum_{\rho=1}^{\iota} \widetilde{\mathcal{A}}_\rho \eta(\iota-\rho)|\mu(\iota)] + \sum_{\rho=0}^{\iota} \widetilde{\mathcal{B}}_\rho u(\iota-\rho). \end{aligned} \tag{14} $$

Supposing that $E[\eta(\iota-\rho)|\mu(\iota)] \cong E[\eta(\iota-\rho)|\sigma(\iota-\rho)]$, we obtain

$$ \widehat{\eta}(\iota|\iota-1) = \sum_{\rho=1}^{\iota} \widetilde{\mathcal{A}}_\rho \widehat{\eta}(\iota-\rho|\iota-\rho) + \sum_{\rho=0}^{\iota} \widetilde{\mathcal{B}}_\rho u(\iota-\rho). \tag{15} $$

Denoting $K(\iota)$ as the Kalman gain matrix, the estimation of $\eta(\iota)$ with the correction term is given by

$$ \widehat{\eta}(\iota|\iota) = \widehat{\eta}(\iota|\iota-1) + K(\iota)(z(\iota) - \widetilde{C}\widehat{\eta}(\iota|\iota-1)). \tag{16} $$

From equations (13) and (15), the estimation error matrix is estimated as

$$ \begin{aligned} &P(\iota|\iota-1) \\ &= E[(\widehat{\eta}(\iota|\iota-1) - \eta(\iota))(\widehat{\eta}(\iota|\iota-1) - \eta(\iota))^T] \\ &= E[(\sum_{\sigma=1}^{\iota} \widetilde{\mathcal{A}}_\sigma (\widehat{\eta}(\iota-\sigma|\iota-\sigma) - \eta(\iota-\sigma)) - \sum_{\sigma=0}^{\iota} \widetilde{\mathcal{H}}_\sigma \varepsilon(\iota-\sigma)) \\ &\quad \times (\sum_{\rho=1}^{\iota} \widetilde{\mathcal{A}}_\rho (\widehat{\eta}(\iota-\rho|\iota-\rho) - \eta(\iota-\rho)) - \sum_{\rho=0}^{\iota} \widetilde{\mathcal{H}}_\rho \varepsilon(\iota-\rho))^T]. \end{aligned} \tag{17} $$

Because the norm of the noise matrix $\widetilde{\mathcal{H}}_\rho$ gets smaller with the increase of ρ, the estimation error $\widehat{\eta}(\iota|\iota) - \eta(\iota)$ can be

approximated by

$$\begin{aligned}
&\widehat{\eta}(\iota|\iota)-\eta(\iota)\\
&\quad=\widehat{\eta}(\iota|\iota-1)+K(\iota)(z(\iota)-\widetilde{\mathcal{C}}\widehat{\eta}(\iota|\iota-1))-\eta(\iota)\\
&\quad=(I-K(\iota)\widetilde{\mathcal{C}})(\widehat{\eta}(\iota|\iota-1)-\eta(\iota))+K(\iota)v(\iota)\\
&\quad\approx(I-K(\iota)\widetilde{\mathcal{C}})(\sum_{\rho=1}^{\iota}\widetilde{\mathcal{A}}_{\rho}(\widehat{\eta}(\iota-\rho|\iota-\rho)-\eta(\iota-\rho))\\
&\qquad-\sum_{\rho=0}^{1}\widetilde{\mathcal{H}}_{\rho}\varepsilon(\iota-\rho))+K(\iota)v(\iota). \qquad (18)
\end{aligned}$$

Supposing $\widehat{\eta}(\iota-\rho|\iota-\rho)\approx\eta(\iota-\rho)$, we have

$$\widehat{\eta}(\iota|\iota)-\eta(\iota)\approx-(I-K(\iota)\widetilde{\mathcal{C}})\sum_{\rho=0}^{1}\widetilde{\mathcal{H}}_{\rho}\varepsilon(\iota-\rho)+K(\iota)v(\iota). \qquad (19)$$

For $\sigma=\rho$, it follows that

$$\begin{aligned}
&E[(\sum_{\sigma=1}^{\iota}\widetilde{\mathcal{A}}_{\sigma}(\widehat{\eta}(\iota-\sigma|\iota-\sigma)-\eta(\iota-\sigma)))\\
&\qquad\times(\sum_{\rho=1}^{\iota}(\widehat{\eta}(\iota-\rho|\iota-\rho)-\eta(\iota-\rho))^{T}\widetilde{\mathcal{A}}_{\rho}^{T})]\\
&\qquad=\sum_{\rho=1}^{\iota}\widetilde{\mathcal{A}}_{\rho}P(\iota-\rho|\iota-\rho)\widetilde{\mathcal{A}}_{\rho}^{T}. \qquad (20)
\end{aligned}$$

For $\sigma\neq\rho$, it also follows from (19) that

$$\begin{aligned}
&\widehat{\eta}(\iota-\sigma|\iota-\sigma)-\eta(\iota-\sigma)\\
&\quad\approx-(I-K(\iota-\sigma)\widetilde{\mathcal{C}})\sum_{\rho=0}^{1}\widetilde{\mathcal{H}}_{\rho}\varepsilon(\iota-\sigma-\rho)\\
&\qquad+K(\iota-\sigma)v(\iota-\sigma),
\end{aligned}$$

then, we have

$$\begin{aligned}
&E[(\sum_{\sigma=1}^{\iota}\widetilde{\mathcal{A}}_{\sigma}(\widehat{\eta}(\iota-\sigma|\iota-\sigma)-\eta(\iota-\sigma)))\\
&\qquad\times(\sum_{\rho=1}^{\iota}(\widehat{\eta}(\iota-\rho|\iota-\rho)-\eta(\iota-\rho))^{T}\widetilde{\mathcal{A}}_{\rho}^{T})]\\
&\quad=E[(\sum_{\sigma=1}^{\iota}\widetilde{\mathcal{A}}_{\sigma}(-(I-K(\iota-\sigma)\widetilde{\mathcal{C}})\sum_{\rho=0}^{1}\widetilde{\mathcal{H}}_{\rho}\varepsilon(\iota-\sigma-\rho)\\
&\qquad+K(\iota-\sigma)v(\iota-\sigma)))(\sum_{\rho=1}^{\iota}(-(I-K(\iota-\rho)\widetilde{\mathcal{C}})\\
&\qquad\times\sum_{\rho=0}^{1}\widetilde{\mathcal{H}}_{\rho}\varepsilon(\iota-\rho-\rho)+K(\iota-\rho)v(\iota-\rho))^{T}\widetilde{\mathcal{A}}_{\rho}^{T})]\\
&\quad=E[(\sum_{\sigma=1}^{\iota}(-\widetilde{\mathbf{A}}_{\sigma})(\widetilde{\mathcal{H}}_{0}\varepsilon(\iota-\sigma)+\widetilde{\mathcal{H}}_{1}\varepsilon(\iota-\sigma-1))\\
&\qquad+\sum_{\sigma=1}^{\iota}(-\mathcal{K}_{\sigma})v(\iota-\sigma))(\sum_{\rho=1}^{\iota}(\widetilde{\mathcal{H}}_{0}\varepsilon(\iota-\rho)\\
&\qquad+\widetilde{\mathcal{H}}_{1}\varepsilon(\iota-\rho-1))^{T}(-\widetilde{\mathbf{A}}_{\rho})^{T}+\sum_{\rho=1}^{\iota}v(\iota-\rho)^{T}(-\mathcal{K}_{\rho})^{T})]\\
&\quad\approx\sum_{\rho=1}^{\iota-1}\widetilde{\mathbf{A}}_{\rho}\widetilde{\mathcal{H}}_{1}Q\widetilde{\mathcal{H}}_{0}^{T}\widetilde{\mathbf{A}}_{\rho+1}^{T}+\sum_{\rho=1}^{\iota-1}\widetilde{\mathbf{A}}_{\rho+1}\widetilde{\mathcal{H}}_{0}Q\widetilde{\mathcal{H}}_{1}^{T}\widetilde{\mathbf{A}}_{\rho}^{T}\\
&\qquad+\sum_{\rho=1}^{\iota-1}\widetilde{\mathbf{A}}_{\rho}\widetilde{\mathcal{H}}_{1}\mathcal{W}\mathcal{K}_{\rho+1}^{T}+\sum_{\rho=1}^{\iota-1}\mathcal{K}_{\rho+1}\mathcal{W}^{T}\widetilde{\mathcal{H}}_{1}^{T}\widetilde{\mathbf{A}}_{\rho}^{T}, \qquad (21)
\end{aligned}$$

where $\widetilde{\mathbf{A}}_{\rho}=\widetilde{\mathcal{A}}_{\rho}(I-K(\iota-\rho)\widetilde{\mathcal{C}})$, $\mathcal{K}_{\rho}=-\widetilde{\mathcal{A}}_{\rho}K(\iota-\rho)$, and $K(\iota-\rho)$ in $\widetilde{\mathbf{A}}_{\rho}$ represents the Kalman gain matrix starting from the ιth iteration and pushing forward the ρth iteration.

Meanwhile, we also have

$$\begin{aligned}
&E[(\sum_{\sigma=1}^{\iota}\widetilde{\mathcal{A}}_{\sigma}(\widehat{\eta}(\iota-\sigma|\iota-\sigma)-\eta(\iota-\sigma)))(\sum_{\rho=0}^{\iota}\widetilde{\mathcal{H}}_{\rho}\varepsilon(\iota-\rho))^{T}]\\
&=E[(\sum_{\sigma=1}^{\iota}\widetilde{\mathcal{A}}_{\sigma}(-(I-K(\iota-\sigma)\widetilde{\mathcal{C}})\sum_{\rho=0}^{1}\widetilde{\mathcal{H}}_{\rho}\varepsilon(\iota-\sigma-\rho)\\
&\qquad+K(\iota-\sigma)v(\iota-\sigma)))(\sum_{\rho=0}^{\iota}\widetilde{\mathcal{H}}_{\rho}\varepsilon(\iota-\rho))^{T}]\\
&=E[(\sum_{\sigma=1}^{\iota}(-\widetilde{\mathbf{A}}_{\sigma})(\widetilde{\mathcal{H}}_{0}\varepsilon(\iota-\sigma)+\widetilde{\mathcal{H}}_{1}\varepsilon(\iota-\sigma-1))\\
&\qquad+\sum_{\sigma=1}^{\iota}(-\mathcal{K}_{\sigma})v(\iota-\sigma))(\sum_{\rho=0}^{\iota}\widetilde{\mathcal{H}}_{\rho}\varepsilon(\iota-\rho))^{T}]\\
&\approx-\sum_{\rho=1}^{\iota}\widetilde{\mathbf{A}}_{\rho}\widetilde{\mathcal{H}}_{0}Q\widetilde{\mathcal{H}}_{\rho}^{T}-\sum_{\rho=1}^{\iota-1}\widetilde{\mathbf{A}}_{\rho}\widetilde{\mathcal{H}}_{1}Q\widetilde{\mathcal{H}}_{\rho+1}^{T}-\sum_{\rho=1}^{\iota}\mathcal{K}_{\rho}\mathcal{W}^{T}\widetilde{\mathcal{H}}_{\rho}^{T}, \qquad (22)
\end{aligned}$$

$$\begin{aligned}
&E[(\sum_{\sigma=0}^{\iota}\widetilde{\mathcal{H}}_{\sigma}\varepsilon(\iota-\sigma))(\sum_{\rho=1}^{\iota}\widetilde{\mathcal{A}}_{\rho}(\widehat{\eta}(\iota-\rho|\iota-\rho)-\eta(\iota-\rho)))^{T}]\\
&=E[(\sum_{\sigma=0}^{\iota}\widetilde{\mathcal{H}}_{\sigma}\varepsilon(\iota-\sigma))(\sum_{\rho=1}^{\iota}(-(I-K(\iota-\rho)\widetilde{\mathcal{C}})\\
&\qquad\times\sum_{\rho=0}^{1}\widetilde{\mathcal{H}}_{\rho}\varepsilon(\iota-\rho-\rho)+K(\iota-\rho)v(\iota-\rho))^{T}\widetilde{\mathcal{A}}_{\rho}^{T})]\\
&=E[(\sum_{\sigma=0}^{\iota}\widetilde{\mathcal{H}}_{\sigma}\varepsilon(\iota-\sigma))(\sum_{\rho=1}^{\iota}(\widetilde{\mathcal{H}}_{0}\varepsilon(\iota-\rho)\\
&\qquad+\widetilde{\mathcal{H}}_{1}\varepsilon(\iota-\rho-1))^{T}(-\widetilde{\mathbf{A}}_{\rho})^{T}+\sum_{\rho=1}^{\iota}v(\iota-\rho)^{T}(-\mathcal{K}_{\rho})^{T})]\\
&\approx-\sum_{\rho=1}^{\iota}\widetilde{\mathcal{H}}_{\rho}Q\widetilde{\mathcal{H}}_{0}^{T}\widetilde{\mathbf{A}}_{\rho}^{T}-\sum_{\rho=1}^{\iota-1}\widetilde{\mathcal{H}}_{\rho+1}Q\widetilde{\mathcal{H}}_{1}^{T}\widetilde{\mathbf{A}}_{\rho}^{T}-\sum_{\rho=1}^{\iota}\widetilde{\mathcal{H}}_{\rho}\mathcal{W}\mathcal{K}_{\rho}^{T}, \qquad (23)
\end{aligned}$$

and

$$E[(\sum_{\sigma=0}^{\iota}\widetilde{\mathcal{H}}_{\sigma}\varepsilon(\iota-\sigma))(\sum_{\rho=0}^{\iota}\widetilde{\mathcal{H}}_{\rho}\varepsilon(\iota-\rho))^{T}]=\sum_{\rho=0}^{\iota}\widetilde{\mathcal{H}}_{\rho}Q\widetilde{\mathcal{H}}_{\rho}^{T}. \qquad (24)$$

According to equations (14)-(24), we offer the following FOKF to carry out a satisfactory estimation of the state information for the investigated FOS with the correlated colored process noise.

Theorem 1: For a continuous-time linear FOS described by (2) and (3) with correlated noises $w(\iota)$ and $v(\iota)$, where $w(\iota)$ is the fractional-order colored noise, $v(\iota)$ is the white Gaussian noise, the FOKF based on TGF is designed as follows

$$\begin{aligned}
\widehat{\eta}(\iota|\iota-1) &= \sum_{\rho=1}^{\iota}\widetilde{\mathcal{A}}_\rho\widehat{\eta}(\iota-\rho|\iota-\rho)+\sum_{\rho=0}^{\iota}\widetilde{\mathcal{B}}_\rho u(\iota-\rho),\\
\widehat{\eta}(\iota|\iota) &= \widehat{\eta}(\iota|\iota-1)+K(\iota)(z(\iota)-\widetilde{\mathcal{C}}\widehat{\eta}(\iota|\iota-1)),\\
P(\iota|\iota-1)&\\
&=\sum_{\rho=1}^{\iota}\widetilde{\mathcal{A}}_\rho P(\iota-\rho|\iota-\rho)\widetilde{\mathcal{A}}_\rho^T+\sum_{\rho=1}^{\iota-1}\widetilde{\mathbf{A}}_\rho\widetilde{\mathcal{H}}_1\mathcal{Q}\widetilde{\mathcal{H}}_0^T\widetilde{\mathbf{A}}_{\rho+1}^T\\
&\quad+\sum_{\rho=1}^{\iota-1}\widetilde{\mathbf{A}}_{\rho+1}\widetilde{\mathcal{H}}_0\mathcal{Q}\widetilde{\mathcal{H}}_1^T\widetilde{\mathbf{A}}_\rho^T+\sum_{\rho=1}^{\iota-1}\widetilde{\mathbf{A}}_\rho\widetilde{\mathcal{H}}_1\mathcal{W}\mathcal{K}_{\rho+1}^T\\
&\quad+\sum_{\rho=1}^{\iota-1}\mathcal{K}_{\rho+1}\mathcal{W}^T\widetilde{\mathcal{H}}_1^T\widetilde{\mathbf{A}}_\rho^T+\sum_{\rho=1}^{\iota}\widetilde{\mathbf{A}}_\rho\widetilde{\mathcal{H}}_0\mathcal{Q}\widetilde{\mathcal{H}}_\rho^T\\
&\quad+\sum_{\rho=1}^{\iota-1}\widetilde{\mathbf{A}}_\rho\widetilde{\mathcal{H}}_1\mathcal{Q}\widetilde{\mathcal{H}}_{\rho+1}^T+\sum_{\rho=1}^{\iota}\mathcal{K}_\rho\mathcal{W}^T\widetilde{\mathcal{H}}_\rho^T\\
&\quad+\sum_{\rho=1}^{\iota}\widetilde{\mathcal{H}}_\rho\mathcal{Q}\widetilde{\mathcal{H}}_0^T\widetilde{\mathbf{A}}_\rho^T\\
&\quad+\sum_{\rho=1}^{\iota-1}\widetilde{\mathcal{H}}_{\rho+1}\mathcal{Q}\widetilde{\mathcal{H}}_1^T\widetilde{\mathbf{A}}_\rho^T+\sum_{\rho=1}^{\iota}\widetilde{\mathcal{H}}_\rho\mathcal{W}\mathcal{K}_\rho^T\\
&\quad+\sum_{\rho=0}^{\iota}\widetilde{\mathcal{H}}_\rho\mathcal{Q}\widetilde{\mathcal{H}}_\rho^T,\\
K(\iota) &= (P(\iota|\iota-1)\widetilde{\mathcal{C}}^T+\widetilde{\mathcal{H}}_0\mathcal{W})(\widetilde{\mathcal{C}}P(\iota|\iota-1)\widetilde{\mathcal{C}}^T\\
&\quad+\mathcal{W}^T\widetilde{\mathcal{H}}_0^T\widetilde{\mathcal{C}}^T+\widetilde{\mathcal{C}}\widetilde{\mathcal{H}}_0\mathcal{W}+R)^{-1},\\
P(\iota|\iota) &= (I-K(\iota)\widetilde{\mathcal{C}})P(\iota|\iota-1)(I-K(\iota)\widetilde{\mathcal{C}})^T\\
&\quad+K(\iota)(\widetilde{\mathcal{C}}\widetilde{\mathcal{H}}_0\mathcal{W}+\mathcal{W}^T\widetilde{\mathcal{H}}_0^T\widetilde{\mathcal{C}}^T+R)K^T(\iota)\\
&\quad-\widetilde{\mathcal{H}}_0\mathcal{W}K^T(\iota)-K(\iota)\mathcal{W}^T\widetilde{\mathcal{H}}_0^T.
\end{aligned}$$

Proof: Substituting (18)-(24) into (17), we get the estimation error matrix $P(\iota|\iota-1)$.

By using the equation (18), it follows that

$$\begin{aligned}
P(\iota|\iota) &= E[(\widehat{\eta}(\iota|\iota)-\eta(\iota))(\widehat{\eta}(\iota|\iota)-\eta(\iota))^T]\\
&= E[((I-K(\iota)\widetilde{\mathcal{C}})(\widehat{\eta}(\iota|\iota-1)-\eta(\iota))+K(\iota)v(\iota))\\
&\quad\times((I-K(\iota)\widetilde{\mathcal{C}})(\widehat{\eta}(\iota|\iota-1)-\eta(\iota))+K(\iota)v(\iota))^T]\\
&= (I-K(\iota)\widetilde{\mathcal{C}})P(\iota|\iota-1)(I-K(\iota)\widetilde{\mathcal{C}})^T\\
&\quad+K(\iota)(R+\widetilde{\mathcal{C}}\widetilde{\mathcal{H}}_0\mathcal{W}+\mathcal{W}^T\widetilde{\mathcal{H}}_0^T\widetilde{\mathcal{C}}^T)K^T(\iota)\\
&\quad-\widetilde{\mathcal{H}}_0\mathcal{W}K^T(\iota)-K(\iota)\mathcal{W}^T\widetilde{\mathcal{H}}_0^T. \qquad (25)
\end{aligned}$$

In fact, the terms $\partial[(\widehat{\eta}(\iota|\iota)-\eta(\iota))^T(\widehat{\eta}(\iota|\iota)-\eta(\iota))]/\partial K(\iota)=\mathbf{0}$ and $\partial\mathrm{tr}(P(\iota|\iota))/\partial K(\iota)=\mathbf{0}$ are equivalent in [28]. Therefore, we yield

$$\begin{aligned}
&-\widetilde{\mathcal{C}}P(\iota|\iota-1)(I-K(\iota)\widetilde{\mathcal{C}})^T+(\widetilde{\mathcal{C}}\widetilde{\mathcal{H}}_0\mathcal{W}\\
&\qquad+\mathcal{W}^T\widetilde{\mathcal{H}}_0^T\widetilde{\mathcal{C}}^T+R)K^T(\iota)-\mathcal{W}^T\widetilde{\mathcal{H}}_0^T=\mathbf{0}. \qquad (26)
\end{aligned}$$

Then, $K(\iota)$ is yielded as

$$\begin{aligned}
K(\iota) &= (P(\iota|\iota-1)\widetilde{\mathcal{C}}^T+\widetilde{\mathcal{H}}_0\mathcal{W})(\widetilde{\mathcal{C}}P(\iota|\iota-1)\widetilde{\mathcal{C}}^T\\
&\quad+\mathcal{W}^T\widetilde{\mathcal{H}}_0^T\widetilde{\mathcal{C}}^T+\widetilde{\mathcal{C}}\widetilde{\mathcal{H}}_0\mathcal{W}+R)^{-1}. \qquad (27)
\end{aligned}$$

Remark 1: If the FOKF gained from Theorem 1 is applied to a practical engineering, we need to concern the limited storage problem for the state and the input information. For $\iota\geq L$, the truncation L is introduced into the prediction $\widehat{\eta}(\iota|\iota-1)$ and the prediction error matrix $P(\iota|\iota-1)$ as

$$\begin{aligned}
&\widehat{\eta}(\iota|\iota-1)\\
&=\sum_{\rho=1}^{L}\widetilde{\mathcal{A}}_\rho\widehat{\eta}(\iota-\rho|\iota-\rho)+\sum_{\rho=0}^{L}\widetilde{\mathcal{B}}_\rho u(\iota-\rho),\\
&P(\iota|\iota-1)\\
&=\sum_{\rho=1}^{L}\widetilde{\mathcal{A}}_\rho P(\iota-\rho|\iota-\rho)\widetilde{\mathcal{A}}_\rho^T+\sum_{\rho=1}^{L-1}\widetilde{\mathbf{A}}_\rho\widetilde{\mathcal{H}}_1\mathcal{Q}\widetilde{\mathcal{H}}_0^T\widetilde{\mathbf{A}}_{\rho+1}^T\\
&\quad+\sum_{\rho=1}^{L-1}\widetilde{\mathbf{A}}_{\rho+1}\widetilde{\mathcal{H}}_0\mathcal{Q}\widetilde{\mathcal{H}}_1^T\widetilde{\mathbf{A}}_\rho^T+\sum_{\rho=1}^{L-1}\widetilde{\mathbf{A}}_\rho\widetilde{\mathcal{H}}_1\mathcal{W}\mathcal{K}_{\rho+1}^T\\
&\quad+\sum_{\rho=1}^{L-1}\mathcal{K}_{\rho+1}\mathcal{W}^T\widetilde{\mathcal{H}}_1^T\widetilde{\mathbf{A}}_\rho^T+\sum_{\rho=1}^{L}\widetilde{\mathbf{A}}_\rho\widetilde{\mathcal{H}}_0\mathcal{Q}\widetilde{\mathcal{H}}_\rho^T\\
&\quad+\sum_{\rho=1}^{L-1}\widetilde{\mathbf{A}}_\rho\widetilde{\mathcal{H}}_1\mathcal{Q}\widetilde{\mathcal{H}}_{\rho+1}^T+\sum_{\rho=1}^{L}\mathcal{K}_\rho\mathcal{W}^T\widetilde{\mathcal{H}}_\rho^T+\sum_{\rho=1}^{L}\widetilde{\mathcal{H}}_\rho\mathcal{Q}\widetilde{\mathcal{H}}_0^T\widetilde{\mathbf{A}}_\rho^T\\
&\quad+\sum_{\rho=1}^{L-1}\widetilde{\mathcal{H}}_{\rho+1}\mathcal{Q}\widetilde{\mathcal{H}}_1^T\widetilde{\mathbf{A}}_\rho^T+\sum_{\rho=1}^{L}\widetilde{\mathcal{H}}_\rho\mathcal{W}\mathcal{K}_\rho^T+\sum_{\rho=0}^{L}\widetilde{\mathcal{H}}_\rho\mathcal{Q}\widetilde{\mathcal{H}}_\rho^T.
\end{aligned}$$

B. TREATMENT ON COLORED MEASUREMENT NOISE PROBLEM

For this case, $w(\iota)$ and $v(\iota)$ are correlated, where $w(\iota)$ is white Gaussian noise with $E[w(\iota)]=\mathbf{0}$ and $E[w(\iota)w^T(\kappa)]=M\delta(\iota-\kappa)$, and $v(\tau)$ is the fractional-order colored noise satisfying the following equation

$$_0^C D_\tau^\gamma v(\tau)=Sv(\tau)+D\xi(\tau), \qquad (28)$$

where $\gamma\in(0,2)$, $S\in\mathbb{R}^{q\times q}$, $D\in\mathbb{R}^{q\times\tau}$. The sampling value $\xi(\iota)\in\mathbb{R}^\tau$ is the white Gaussian noise with $E[\xi(\iota)]=\mathbf{0}$, $E[\xi(\iota)\xi^T(\kappa)]=N\delta(\iota-\kappa)$ and $E[w(\iota)\xi^T(\kappa)]=\overline{L}\delta(\iota-\kappa)\neq\mathbf{0}$, M is a positive semidefinite matrix and N is a positive definite matrix.

Similarly, $v(\tau)$ is discretized as

$$(\frac{2}{T})^\gamma(\frac{1-p^{-1}}{1+p^{-1}})^\gamma v(\iota)=Sv(\iota)+D\xi(\iota). \qquad (29)$$

Then, we have

$$(\frac{2}{T})^{\gamma}\sum_{\rho=0}^{\iota}(-1)^{\rho}\binom{\gamma}{\rho}v(\iota-\rho) = \sum_{\rho=0}^{\iota}\binom{\gamma}{\rho}(Sv(\iota-\rho)+D\xi(\iota-\rho)). \quad (30)$$

For simplifying calculations, we define the following matrices as

$$\mathcal{S}_{\rho} = \left((\frac{2}{T})^{\gamma}I - S\right)^{-1}\binom{\gamma}{\rho}\left[(-1)^{\rho+1}(\frac{2}{T})^{\gamma}I + S\right],$$
$$\mathcal{D}_{\rho} = \left((\frac{2}{T})^{\gamma}I - S\right)^{-1}\binom{\gamma}{\rho}D.$$

Therefore, we obtain

$$v(\iota) = \sum_{\rho=1}^{\iota}\mathcal{S}_{\rho}v(\iota-\rho) + \sum_{\rho=0}^{\iota}\mathcal{D}_{\rho}\xi(\iota-\rho). \quad (31)$$

Defining the augmented state and augmented noise as $\varsigma(\iota) = [x^T(\iota), v^T(\iota)]^T$ and $\zeta(\iota) = [w^T(\iota), \xi^T(\iota)]^T$ respectively, the augmented system is represented by

$$\varsigma(\iota) = \sum_{\rho=1}^{\iota}\overline{\mathcal{A}}_{\rho}\varsigma(\iota-\rho) + \sum_{\rho=0}^{\iota}\overline{\mathcal{B}}_{\rho}u(\iota-\rho) + \sum_{\rho=0}^{\iota}\overline{\mathcal{D}}_{\rho}\zeta(\iota-\rho), \quad (32)$$

where $\overline{\mathcal{A}}_{\rho} = \begin{bmatrix}\mathcal{A}_{\rho} & \mathbf{0}\\ \mathbf{0} & \mathcal{S}_{\rho}\end{bmatrix}$, $\overline{\mathcal{B}}_{\rho} = \begin{bmatrix}\mathcal{B}_{\rho}\\ \mathbf{0}\end{bmatrix}$ and $\overline{\mathcal{D}}_{\rho} = \begin{bmatrix}\mathcal{G}_{\rho} & \mathbf{0}\\ \mathbf{0} & \mathcal{D}_{\rho}\end{bmatrix}$.

Consequently, the output equation is transformed into $z(\iota) = \overline{\mathcal{C}}\varsigma(\iota)$, where $\overline{\mathcal{C}} = [C, I]$.

The the covariance matrix and mathematical expectation of the augmented noise satisfy $E[\zeta(\iota)\zeta^T(\iota)] = \overline{\mathcal{W}} = \begin{bmatrix}M & \overline{L}\\ \overline{L}^T & N\end{bmatrix}$ and $E[\zeta(\iota)] = \mathbf{0}$. Since $\overline{\mathcal{W}}$ is required to be a positive semidefinite matrix, the condition $\overline{\mathcal{W}} \geq \mathbf{0}$ can be achieved by $N - \overline{L}^T M^{-1}\overline{L} \geq \mathbf{0}$ according to the [31].

The estimation of $\varsigma(\iota)$ satisfying $\widehat{\varsigma}(\iota|\iota) = E[\varsigma(\iota)|\sigma(\iota)]$ is defined, where $\sigma(\iota)$ includes the information of $z(0)$, $z(1)$, …, $z(\iota)$, $u(0)$, $u(1)$, …, $u(\iota)$. Besides, the predication of $\varsigma(\iota)$ satisfying $\widehat{\varsigma}(\iota|\iota-1) = E[\varsigma(\iota)|\mu(\iota)]$ is defined, where $\mu(\iota)$ includes $z(0)$, $z(1)$, …, $z(\iota-1)$, $u(0)$, $u(1)$, …, $u(\iota)$.

By using the same method via equations (14) and (15), the prediction $\widehat{\varsigma}(\iota|\iota-1)$ is got by

$$\begin{aligned}\widehat{\varsigma}(\iota|\iota-1) &= E[(\sum_{\rho=1}^{\iota}\overline{\mathcal{A}}_{\rho}\varsigma(\iota-\rho) + \sum_{\rho=0}^{\iota}\overline{\mathcal{B}}_{\rho}u(\iota-\rho) + \sum_{\rho=0}^{\iota}\overline{\mathcal{D}}_{\rho}\zeta(\iota-\rho))|\mu(\iota)]\\ &= E[(\sum_{\rho=1}^{\iota}\overline{\mathcal{A}}_{\rho}\varsigma(\iota-\rho))|\mu(\iota)] + \sum_{\rho=0}^{\iota}\overline{\mathcal{B}}_{\rho}u(\iota-\rho)\\ &= \sum_{\rho=1}^{\iota}\overline{\mathcal{A}}_{\rho}\widehat{\varsigma}(\iota-\rho|\iota-\rho) + \sum_{\rho=0}^{\iota}\overline{\mathcal{B}}_{\rho}u(\iota-\rho).\end{aligned} \quad (33)$$

Then, we can get

$$\begin{aligned}&\widehat{\varsigma}(\iota|\iota-1) - \varsigma(\iota)\\ &= \sum_{\rho=1}^{\iota}\overline{\mathcal{A}}_{\rho}(\widehat{\varsigma}(\iota-\rho|\iota-\rho) - \varsigma(\iota-\rho)) - \sum_{\rho=0}^{\iota}\overline{\mathcal{D}}_{\rho}\zeta(\iota-\rho).\end{aligned} \quad (34)$$

The estimation of $\varsigma(\iota)$ is represented by

$$\widehat{\varsigma}(\iota|\iota) = \widehat{\varsigma}(\iota|\iota-1) + K(\iota)(z(\iota) - \overline{\mathcal{C}}\widehat{\varsigma}(\iota|\iota-1)). \quad (35)$$

Supposing $\widehat{\varsigma}(\iota-\rho|\iota-\rho) \approx \varsigma(\iota-\rho)$, we obtain

$$\begin{aligned}&\widehat{\varsigma}(\iota|\iota) - \varsigma(\iota)\\ &= \widehat{\varsigma}(\iota|\iota-1) + K(\iota)(z(\iota) - \overline{\mathcal{C}}\widehat{\varsigma}(\iota|\iota-1)) - \varsigma(\iota)\\ &= (I - K(\iota)\overline{\mathcal{C}})(\widehat{\varsigma}(\iota|\iota-1) - \varsigma(\iota))\\ &= (I - K(\iota)\overline{\mathcal{C}})(\sum_{\rho=1}^{\iota}\overline{\mathcal{A}}_{\rho}(\widehat{\varsigma}(\iota-\rho|\iota-\rho) - \varsigma(\iota-\rho))\\ &\quad - \sum_{\rho=0}^{\iota}\overline{\mathcal{D}}_{\rho}\zeta(\iota-\rho))\\ &\approx -(I - K(\iota)\overline{\mathcal{C}})\sum_{\rho=0}^{1}\overline{\mathcal{D}}_{\rho}\zeta(\iota-\rho).\end{aligned} \quad (36)$$

For $\sigma \neq \rho$, it follows that

$$\begin{aligned}&E[(\sum_{\sigma=1}^{\iota}\overline{\mathcal{A}}_{\sigma}(\widehat{\varsigma}(\iota-\sigma|\iota-\sigma) - \varsigma(\iota-\sigma)))\\ &\quad\times(\sum_{\rho=1}^{\iota}(\widehat{\varsigma}(\iota-\rho|\iota-\rho) - \varsigma(\iota-\rho))^T\overline{\mathcal{A}}_{\rho}^T)]\\ &\approx \sum_{\rho=1}^{\iota-1}\overline{\mathbf{A}}_{\rho}\overline{\mathcal{D}}_1\,\overline{\mathcal{W}}\,\overline{\mathcal{D}}_0^T\overline{\mathbf{A}}_{\rho+1}^T + \sum_{\rho=1}^{\iota-1}\overline{\mathbf{A}}_{\rho+1}\overline{\mathcal{D}}_0\,\overline{\mathcal{W}}\,\overline{\mathcal{D}}_1^T\overline{\mathbf{A}}_{\rho}^T,\end{aligned} \quad (37)$$

where $\overline{\mathbf{A}}_{\rho} = \overline{\mathcal{A}}_{\rho}(I - K(\iota-\rho)\overline{\mathcal{C}})$.

Besides, it also follows that

$$\begin{aligned}&E[(\sum_{\sigma=1}^{\iota}\overline{\mathcal{A}}_{\sigma}(\widehat{\varsigma}(\iota-\sigma|\iota-\sigma) - \varsigma(\iota-\sigma)))(\sum_{\rho=0}^{\iota}\overline{\mathcal{D}}_{\rho}\zeta(\iota-\rho))^T]\\ &\approx -\sum_{\rho=1}^{\iota}\overline{\mathbf{A}}_{\rho}\overline{\mathcal{D}}_0\,\overline{\mathcal{W}}\,\overline{\mathcal{D}}_{\rho}^T - \sum_{\rho=1}^{\iota-1}\overline{\mathbf{A}}_{\rho}\overline{\mathcal{D}}_1\,\overline{\mathcal{W}}\,\overline{\mathcal{D}}_{\rho+1}^T.\end{aligned} \quad (38)$$

To cope with problem on the correlated colored measurement noise and white Gaussian process noise, we give the design method of FOKF via TGF to gain an effective state estimation in the following theorem.

Theorem 2: For a continuous-time linear FOS described by (2) and (3) with the correlated noises $w(\iota)$ and $v(\iota)$, where $w(\iota)$ is the white Gaussian noise, $v(\iota)$ is the fractional-order colored noise, the FOKF based on TGF is designed as

follows

$$\widehat{\varsigma}(\iota|\iota-1)=\sum_{\rho=1}^{\iota}\overline{\mathcal{A}}_\rho\widehat{\varsigma}(\iota-\rho|\iota-\rho)+\sum_{\rho=0}^{\iota}\overline{\mathcal{B}}_\rho u(\iota-\rho),$$
$$\widehat{\varsigma}(\iota|\iota)=\widehat{\varsigma}(\iota|\iota-1)+K(\iota)(z(\iota)-\overline{\mathcal{C}}\widehat{\varsigma}(\iota|\iota-1)),$$
$$\begin{aligned}P(\iota|\iota-1)&=\sum_{\rho=1}^{\iota}\overline{\mathcal{A}}_\rho P(\iota-\rho|\iota-\rho)\overline{\mathcal{A}}_\rho^T+\sum_{\rho=1}^{\iota-1}\overline{\mathbf{A}}_\rho\overline{\mathcal{D}}_1\,\overline{\mathcal{W}}\,\overline{\mathcal{D}}_0^T\overline{\mathbf{A}}_{\rho+1}^T\\&+\sum_{\rho=1}^{\iota-1}\overline{\mathbf{A}}_{\rho+1}\overline{\mathcal{D}}_0\,\overline{\mathcal{W}}\,\overline{\mathcal{D}}_1^T\overline{\mathbf{A}}_\rho^T+\sum_{\rho=1}^{\iota}\overline{\mathbf{A}}_\rho\overline{\mathcal{D}}_0\,\overline{\mathcal{W}}\,\overline{\mathcal{D}}_\rho^T\\&+\sum_{\rho=1}^{\iota-1}\overline{\mathbf{A}}_\rho\overline{\mathcal{D}}_1\,\overline{\mathcal{W}}\,\overline{\mathcal{D}}_{\rho+1}^T+\sum_{\rho=1}^{\iota}\overline{\mathcal{D}}_\rho\,\overline{\mathcal{W}}\,\overline{\mathcal{D}}_0^T\overline{\mathbf{A}}_\rho^T\\&+\sum_{\rho=1}^{\iota-1}\overline{\mathcal{D}}_{\rho+1}\,\overline{\mathcal{W}}\,\overline{\mathcal{D}}_1^T\overline{\mathbf{A}}_\rho^T+\sum_{\rho=0}^{\iota}\overline{\mathcal{D}}_\rho\,\overline{\mathcal{W}}\,\overline{\mathcal{D}}_\rho^T,\end{aligned}$$
$$K(\iota)=P(\iota|\iota-1)\overline{\mathcal{C}}^T(\overline{\mathcal{C}}P(\iota|\iota-1)\overline{\mathcal{C}}^T)^{-1},$$
$$P(\iota|\iota)=(I-K(\iota)\overline{\mathcal{C}})P(\iota|\iota-1)(I-K(\iota)\overline{\mathcal{C}})^T.$$

Proof: The proof results are easily proved according to that of Theorem 1. Therefore, the proof process is ignored.

Remark 2: If we apply the FOKF gained from Theorem 2 to a practical engineering, $\widehat{\varsigma}(\iota|\iota-1)$ and $P(\iota|\iota-1)$ can be replaced by the following equations with truncation L. For $\iota\geq L$, $\widehat{\varsigma}(\iota|\iota-1)$ and $P(\iota|\iota-1)$ are rewritten by

$$\widehat{\varsigma}(\iota|\iota-1)=\sum_{\rho=1}^{L}\overline{\mathcal{A}}_\rho\widehat{\varsigma}(\iota-\rho|\iota-\rho)+\sum_{\rho=0}^{L}\overline{\mathcal{B}}_\rho u(\iota-\rho),$$
$$\begin{aligned}P(\iota|\iota-1)&=\sum_{\rho=1}^{L}\overline{\mathcal{A}}_\rho P(\iota-\rho|\iota-\rho)\overline{\mathcal{A}}_\rho^T+\sum_{\rho=1}^{L-1}\overline{\mathbf{A}}_\rho\overline{\mathcal{D}}_1\,\overline{\mathcal{W}}\,\overline{\mathcal{D}}_0^T\overline{\mathbf{A}}_{\rho+1}^T\\&+\sum_{\rho=1}^{L-1}\overline{\mathbf{A}}_{\rho+1}\overline{\mathcal{D}}_0\,\overline{\mathcal{W}}\,\overline{\mathcal{D}}_1^T\overline{\mathbf{A}}_\rho^T+\sum_{\rho=1}^{L}\overline{\mathbf{A}}_\rho\overline{\mathcal{D}}_0\,\overline{\mathcal{W}}\,\overline{\mathcal{D}}_\rho^T\\&+\sum_{\rho=1}^{L-1}\overline{\mathbf{A}}_\rho\overline{\mathcal{D}}_1\,\overline{\mathcal{W}}\,\overline{\mathcal{D}}_{\rho+1}^T+\sum_{\rho=1}^{L}\overline{\mathcal{D}}_\rho\,\overline{\mathcal{W}}\,\overline{\mathcal{D}}_0^T\overline{\mathbf{A}}_\rho^T\\&+\sum_{\rho=1}^{L-1}\overline{\mathcal{D}}_{\rho+1}\,\overline{\mathcal{W}}\,\overline{\mathcal{D}}_1^T\overline{\mathbf{A}}_\rho^T+\sum_{\rho=0}^{L}\overline{\mathcal{D}}_\rho\,\overline{\mathcal{W}}\,\overline{\mathcal{D}}_\rho^T.\end{aligned}$$

IV. SIMULATION EXAMPLES

Example 1: Consider the following FOS with the correlated noises $w(\tau)$ and $v(\tau)$ as

$${}_0^C D_\tau^\alpha x(\tau)=Ax(\tau)+Bu(\tau)+Gw(\tau),\quad(39)$$
$$z(\tau)=Cx(\tau)+v(\tau),\quad(40)$$
$${}_0^C D_\tau^\beta w(\tau)=Fw(\tau)+H\varepsilon(\tau),\quad(41)$$

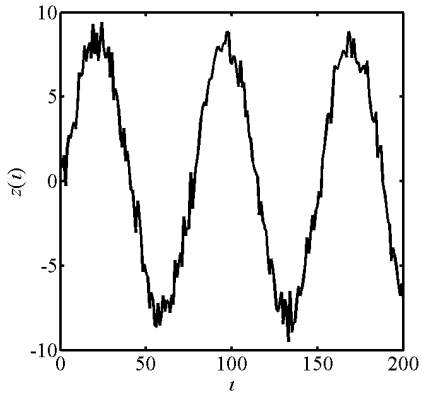

FIGURE 1. $z(\iota)$ in Example 1.

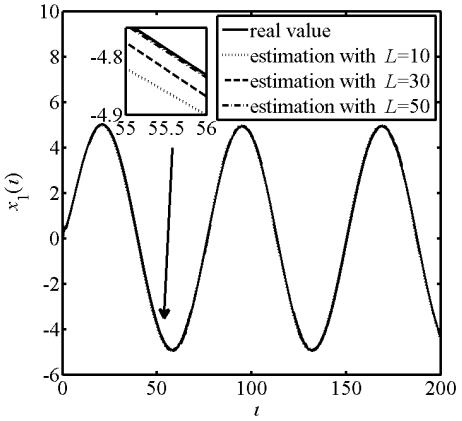

FIGURE 2. $x_1(\iota)$ and its estimations via TGF in Example 1.

where $x(\tau)=[x_1(\tau),x_2(\tau)]^T$, $x(0)=[0.6,-0.5]^T$, $w(0)=0$, $\alpha=0.8$, $\beta=0.6$, $A=\begin{bmatrix}-5&2\\3&-10\end{bmatrix}$, $B=[1,1]^T$, $G=[1,1]^T$, $C=[1,1]$, $Q=0.5$, $R=0.7$, $W=0.2$, $F=-0.5$ and $H=0.2$.

The parameter T is set as $T=0.085$s and 17s is set for the running time. The initial conditions of FOKF are selected as $\widehat{\eta}(0|0)=[0,0,0]^T$, $P(0|0)=I$ and $K(0)=[0,0,0]^T$ in Theorem 1. The input $u(\tau)$ is set as a sine wave function $u(\tau)=20\sin(\tau)$ with the purpose to get the sampling values. Then, $z(\iota)$ is depicted in Figure 1, the state $x(\iota)$ and its estimation are shown for $L=10$, 30, 50 in Figures 2 and 3.

From Figures 2 and 3, the estimations of the state get closer to the real values as the truncation L increases. Hence, the FOKF designed by Theorem 1 based on TGF can estimate the state effectively.

To obtain the comparison results of estimation accuracy via TGF and GLD for different truncations L, the error criterion is defined as

$$E=\frac{1}{H_m+1}\sum_{\iota=0}^{H_m}\sqrt{\sum_{\rho=1}^{2}(\eta_\rho(\iota)-\widehat{\eta}_\rho(\iota|\iota))^2},\quad(42)$$

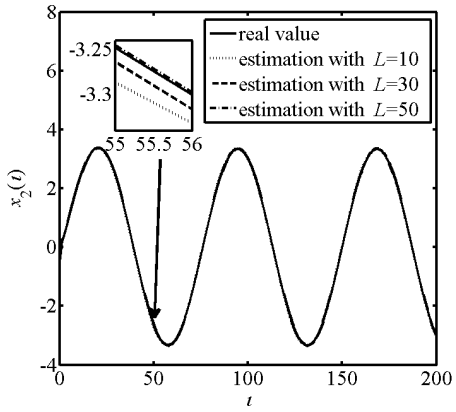

FIGURE 3. $x_2(\iota)$ and its estimations via TGF in Example 1.

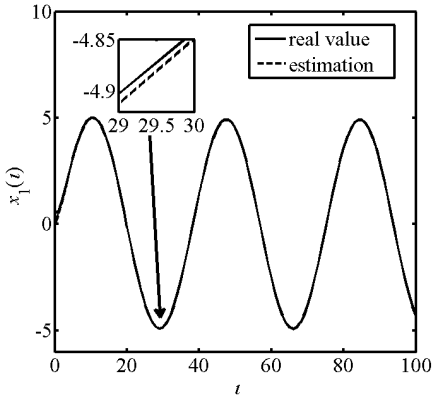

FIGURE 4. $x_1(\iota)$ and its estimation via TGF in Example 1.

TABLE 1. Estimation errors for different truncations in Example 1.

L	TGF	GLD
10	0.10056	0.10717
20	0.04418	0.08639
30	0.02920	0.07650
40	0.02449	0.06624
50	0.02123	0.05794
60	0.01802	0.05452

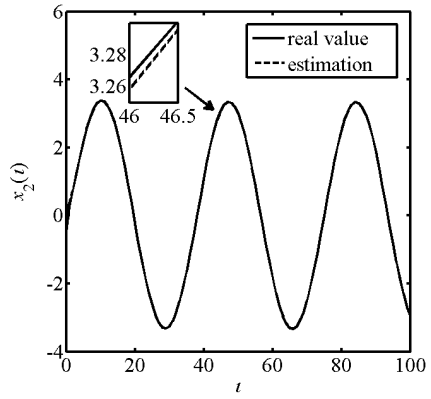

FIGURE 5. $x_2(\iota)$ and its estimation via TGF in Example 1.

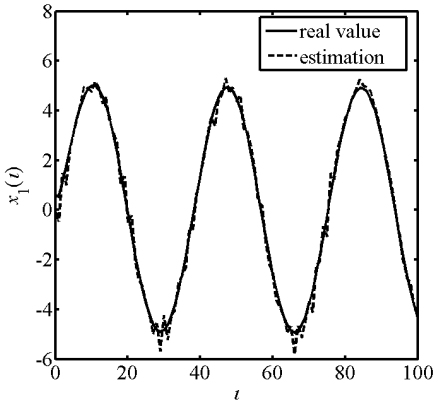

FIGURE 6. $x_1(\iota)$ and its estimation via GLD in Example 1.

where $\eta_1(\iota) = x_1(\iota)$, $\eta_2(\iota) = x_2(\iota)$, $H_m + 1$ is the number of input and output sampling data with $H_m = 200$ for Example 1.

The comparisons with respect to the criterion E via TGF and GLD are given in Table 1 for the truncations $L = 10, 20, \cdots, 60$.

From Table 1, it is seen that the FOKFs via the two types of algorithms are both effective to estimate the state information for the FOS determined by (39), (40) and (41). For $T = 0.085$s, the estimation effect of the FOKF based on TGF is better than that based on GLD for each truncation L. Moreover, the estimation errors of the two algorithms decrease with the increase of L in Table 1. Therefore, it is necessary to consider the estimation error accuracy and computational complexity to select the appropriate truncation L.

The sampling period T is increased to $T = 0.17$s with $L = 30$ and other parameters remain changed, the real values and the estimations of FOS in this example by using TGF and GLD are drawn in Figures 4-7, respectively.

The estimations $\widehat{x}_1(\iota|\iota)$ and $\widehat{x}_2(\iota|\iota)$ by using TGF almost converge the real values $x_1(\iota)$ and $x_2(\iota)$ in Figures 4 and 5, the comparison results illustrate the FOKF proposed by Theorem 1 still can estimate state information effectively, but that performance based on FOKF using GLD is poor. To compare the error indexes of the two types of FOKFs for different sampling periods with $L = 30$, the relationship between E and T from 0.01s to 1s with the step 0.01s is shown in Figure 8.

From Figure 8, we know that two types of FOKFs corresponding to small sampling period can effectively estimate the state information. The method of TGF can obtain the effective estimation state if T increases, but the method with GLD does not work. That is to say, the algorithm proposed in this paper is more applicable to the sampling period. To investigate the effect of the proposed algorithm via Theorem 1 on the estimation of the colored noise with the different fractional-orders β, the comparison results with $L = 30$ and $T = 0.085$s are shown in Table 2.

The results in Table 2 show that both of FOKFs can obtain effective estimation errors for different fractional-orders, but

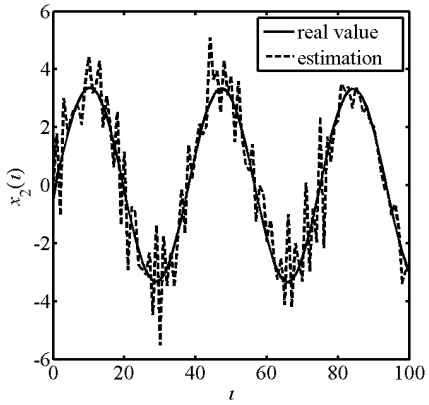

FIGURE 7. $x_2(\iota)$ and its estimation via GLD in Example 1.

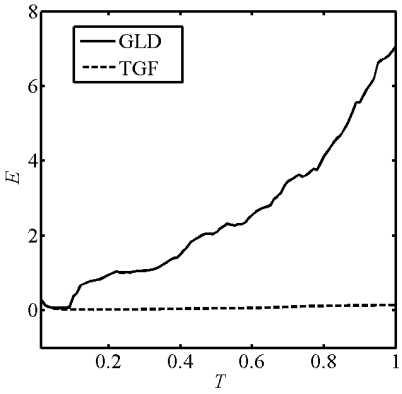

FIGURE 8. Estimation errors for difference T in Example 1.

TABLE 2. Estimation errors for different fractional-orders β in Example 1.

β	TGF	GLD
0.2	0.03009	0.07635
0.3	0.02980	0.07629
0.4	0.02958	0.07631
0.5	0.02939	0.07637
0.6	0.02920	0.07649
0.7	0.02888	0.07674
0.8	0.02824	0.07739

TABLE 3. Estimation errors for different correlation matrices W in Example 1.

W	TGF	GLD
0	0.02878	0.07838
0.1	0.02935	0.07751
0.2	0.02920	0.07649
0.3	0.02897	0.07541
0.4	0.02875	0.07428

the FOKF using TGF in this paper gains smaller errors and higher accuracy than FOKF using GLD method for each fractional-order. It indicates that the proposed algorithm is effective for different fractional-order colored noises. In addition, the correlation matrix W is also concerned to compare with the GLD method using the truncation $L = 30$ and $T = 0.085$s, and the corresponding results are offered in Table 3.

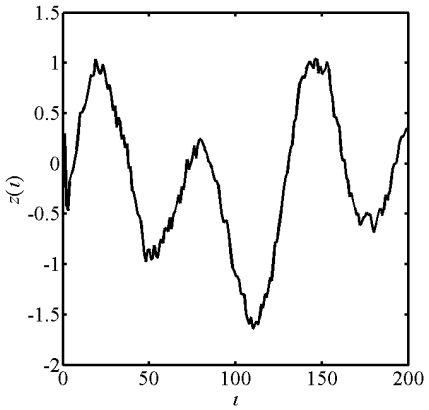

FIGURE 9. $z(\iota)$ in Example 2.

For different correlation matrices W, each estimation error produced by FOKF based on Theorem 1 is less than the corresponding one using GLD method in Table 3. Hence, the FOKF based on the proposed TGF can be applied to different correlated noise cases. Meanwhile, $W = \mathbf{0}$ in Table 3 indicates that the measurement noise and the process noise are not correlated at sampling time. In other words, the proposed algorithm is also applicable to the uncorrelated noises.

Example 2: The measurement noise is concerned as a fractional-order colored noise in this example. Consider the following FOS as

$$
\begin{aligned}
{}_0^C D_\tau^\alpha x(\tau) &= Ax(\tau) + Bu(\tau) + Gw(\tau), && (43)\\
z(\tau) &= Cx(\tau) + v(\tau), && (44)\\
{}_0^C D_\tau^\gamma v(\tau) &= Sv(\tau) + D\xi(\tau), && (45)
\end{aligned}
$$

where $x(\tau) = [x_1(\tau), x_2(\tau)]^T$, $x(0) = [0.8, -1]^T$, $w(0) = 0$, $\alpha = 0.8$, $\gamma = 0.7$, $A = \begin{bmatrix} -25 & 5 \\ 2 & -10 \end{bmatrix}$, $B = [1, 1]^T$, $G = [1, 1]^T$, $C = [1, 0]$, $M = 1$, $N = 1.2$, $\bar{L} = 0.3$, $S = -0.4$ and $D = -0.5$.

The parameter T is set as $T = 0.05$s, and the running time is set as 10s. The initial conditions of the FOKF via Theorem 2 are selected as $\widehat{\eta}(0|0) = [0, 0, 0]^T$, $P(0|0) = I$ and $K(0) = [0, 0, 0]^T$. Meanwhile, the input $u(\tau)$ is set as $u(\tau) = 15\sin(2\tau) - 10\sin(\tau + \pi)$. Besides, $z(\iota)$ is depicted in Figure 9, $x(\iota)$ and its estimation with $L = 10, 30, 50$ are depicted in Figures 10 and 11.

From Figures 10 and 11, it is seen that the estimations using TGF float the real values nearly. Therefore, the proposed FOKF obtains satisfactory state estimations for different truncations L. As the truncation L increases, the estimation value is closer to the real value. We adopt the error index (42) to evaluate the estimation results with $H_m = 200$ for the proposed FOKF via Theorem 2. For different truncations $L = 10, 20, \cdots, 60$, the comparison results of the estimation error produced by TGF and GLD are shown in Table 4.

From Table 4, it is also concluded that the estimation errors E using two types of FOKFs decrease as the truncation L

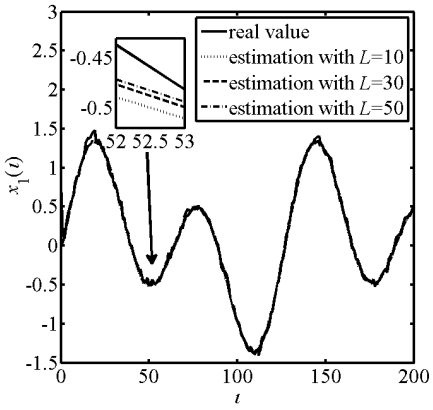

FIGURE 10. $x_1(\iota)$ and its estimations via TGF in Example 2.

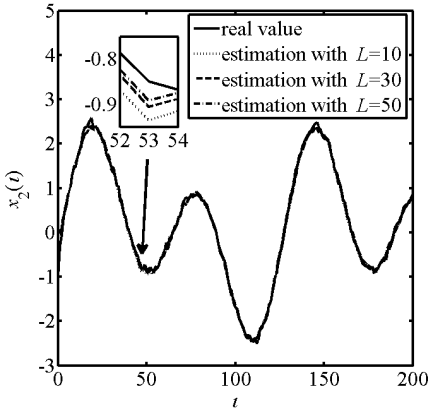

FIGURE 11. $x_2(\iota)$ and its estimations via TGF in Example 2.

TABLE 4. Estimation errors for different truncations L in Example 2.

L	TGF	GLD
10	0.07268	0.11763
20	0.06820	0.11659
30	0.06737	0.11621
40	0.06694	0.11579
50	0.06660	0.11559
60	0.06635	0.11548

increases. For each truncation L, the estimation effect using Theorem 2 is more accurate than GLD method for the FOS described by (43)-(45).

The sampling period is increased to $T = 0.2$s, L is chosen as $L = 30$, and other parameters are not changed, the responses of the real values and estimations of $x_1(\iota)$ and $x_2(\iota)$ are drawn in Figures 12-15.

From the dynamic responses of the estimations and real values shown in Figures 12-15, it can be seen that TGF method can still achieve satisfactory results for the case that the measurement noise is the colored noise for the enlarged sampling period. However, the estimation results obtained by GLD method are very invalid, and the satisfactory state estimation can not be achieved effectively. Similarly, the error indexes E produced by two types of FOKFs for

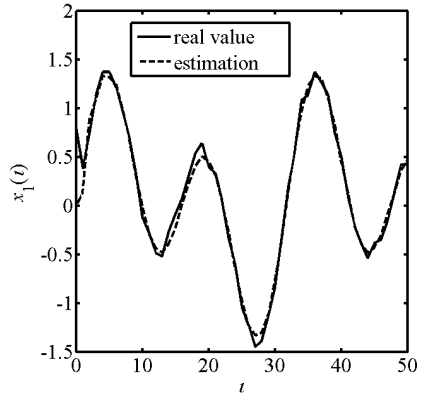

FIGURE 12. $x_1(\iota)$ and its estimation via TGF in Example 2.

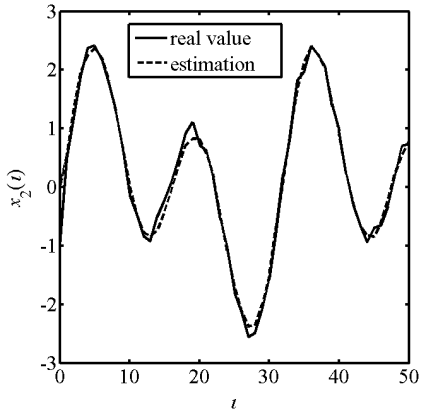

FIGURE 13. $x_2(\iota)$ and its estimation via TGF in Example 2.

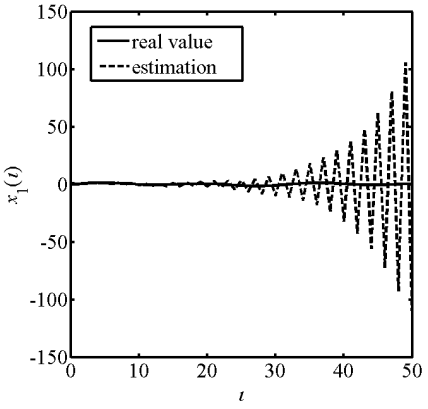

FIGURE 14. $x_1(\iota)$ and its estimation via GLD in Example 2.

$T \in [0.01\text{s}, 0.2\text{s}]$ with the step 0.01s are drawn as shown in Figure 16.

It can be seen clearly that the satisfactory state estimation via GLD method is achieved for a small sampling period. As the sampling period T increases, the method of GLD can not get the effective state estimation. However, the method via TGF is still valid, which is consistent with the conclusion in Example 1.

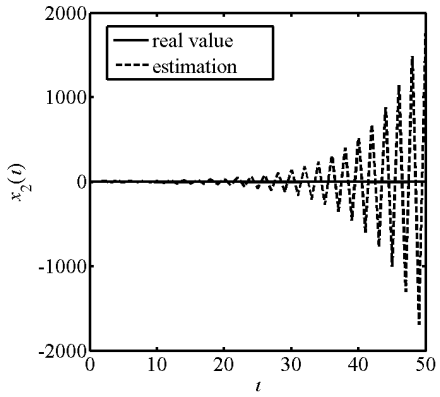

FIGURE 15. $x_2(\iota)$ and its estimation via GLD in Example 2.

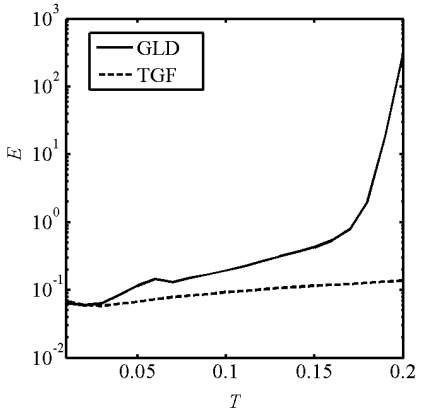

FIGURE 16. Estimation errors for difference T in Example 2.

TABLE 5. Estimation errors for different γ in Example 2.

γ	TGF	GLD
0.2	0.07059	76580.8
0.3	0.07126	0.24985
0.4	0.07227	0.13431
0.5	0.07333	0.11682
0.6	0.07216	0.10859
0.7	0.06737	0.11621
0.8	0.06230	0.12679

TABLE 6. Estimation errors for different $\bar{L}$ in Example 2.

$\bar{L}$	TGF	GLD
0	0.06987	0.12410
0.1	0.06634	0.11915
0.2	0.06667	0.11738
0.3	0.06737	0.11621
0.4	0.06861	0.11530

Besides, we choose the truncation $L = 30$ and the sampling period $T = 0.05$s to discuss the effect of the fractional-order γ and the correlation matrix $\bar{L}$. The comparison results obtained by TGF and GLD are given in Tables 5 and 6, respectively.

From Table 5, the estimation value corresponding to $\gamma = 0.2$ using GLD method is very large, it indicates that the FOKF using GLD fails in this case. Fortunately, the FOKF designed by Theorem 2 can still get the state estimation. Although FOKF based on GLD method can obtain better estimation value for different fractional-orders γ, the FOKF via Theorem 2 obtain the higher estimation accuracy. For different correlation matrices $\bar{L}$, the FOKF provided by Theorem 2 can obtain smaller estimation error, compared with the FOKF designed by GLD method. This conclusion is also true for $\bar{L} = \mathbf{0}$ to validate that Theorem 2 is also applicable to the uncorrelated noise case.

V. CONCLUSION

The problem on state estimation is investigated for continuous-time linear FOSs with the correlated colored noises in this paper. Firstly, the five recursive formulas in FOKF based on TGF are studied to deal with the correlated fractional-order colored process noise, then the case for the correlated colored measurement noise is discussed, similarly.

In fact, the FOKFs via TGF can improve the accuracy of estimation as the truncation increases, compared with GLD. For different the fractional-orders and correlation matrices in colored noises, the effect of state estimation for the investigated FOSs via the proposed KFs based on TGF is better than GLD. And the proposed KFs using TGF still can guarantee the validity of state estimation with the increase of the sampling period for a practical engineering. Thus, the FOKFs based on TGF are more effective and general for state estimation of continuous-time linear FOSs with correlated colored noises. In the future, the proposed algorithms will also be applied to the estimation of practical systems.

REFERENCES

[1] Q. Q. Cheng, P. X. Liu, P. H. Lai, and Y. N. Zou, "An interactive meshless cutting model for nonlinear viscoelastic soft tissue in surgical simulators," *IEEE Access*, vol. 5, pp. 16359–16371, 2017.
[2] G. Iyer and A. Novikov, "Anomalous diffusion in fast cellular flows at intermediate time scales," *Probabillity Theory Rel. Fields*, vol. 164, nos. 3–4, pp. 707–740, Apr. 2016.
[3] J. Fei and C. Lu, "Adaptive fractional order sliding mode controller with neural estimator," *J. Franklin Inst.*, vol. 355, no. 5, pp. 2369–2391, Mar. 2018.
[4] J. Wei, Y. Zhang, and H. Bao, "An exploration on adaptive iterative learning control for a class of commensurate high-order uncertain nonlinear fractional order systems," *IEEE/CAA J. Autom. Sinica*, vol. 5, no. 2, pp. 618–627, Mar. 2018.
[5] B. Hekimoglu, "Optimal tuning of fractional order PID controller for DC motor speed control via chaotic atom search optimization algorithm," *IEEE Access*, vol. 7, pp. 38100–38114, 2019.
[6] S. Y. Shao, M. Chen, and Q. X. Wu, "Tracking control for uncertain fractional-order chaotic systems based on disturbance observer and neural network," *IMA J. Math. Control Inf.*, vol. 34, no. 3, pp. 1011–1030, 2017.
[7] A. Bryson and D. Johansen, "Linear filtering for time-varying systems using measurements containing colored noise," *IEEE Trans. Autom. Control*, vol. AC-10, no. 1, pp. 4–10, Jan. 1965.
[8] Z. Wang, Y. Qin, C. Hu, M. Dong, and F. Li, "Fuzzy observer-based prescribed performance control of vehicle roll behavior via controllable damper," *IEEE Access*, vol. 7, pp. 19471–19487, 2019.
[9] H. Han, Y. Ding, K. Hao, and L. Hu, "Particle filter for state estimation of jump Markov nonlinear system with application to multi-targets tracking," *Int. J. Syst. Sci.*, vol. 44, no. 7, pp. 1333–1343, Jul. 2013.
[10] M. G. Petovello, K. O'Keefe, G. Lachapelle, and M. E. Cannon, "Consideration of time-correlated errors in a Kalman filter applicable to GNSS," *J. Geodesy*, vol. 83, no. 1, pp. 51–56, Jan. 2009.

[11] Y. Wang, Y. Sun, V. Dinavahi, S. Cao, and D. Hou, "Adaptive robust cubature Kalman filter for power system dynamic state estimation against outliers," *IEEE Access*, vol. 7, pp. 105872–105881, 2019.
[12] F. Deng, J. Chen, and C. Chen, "Adaptive unscented Kalman filter for parameter and state estimation of nonlinear high-speed objects," *J. Syst. Eng. Electron.*, vol. 24, no. 4, pp. 655–665, Aug. 2013.
[13] W. Liu, "State estimation for discrete-time Markov jump linear systems with time-correlated measurement noise," *Automatica*, vol. 76, pp. 266–276, Feb. 2017.
[14] W. Liu, P. Shi, and J.-S. Pan, "State estimation for discrete-time Markov jump linear systems with time-correlated and mode-dependent measurement noise," *Automatica*, vol. 85, pp. 9–21, Nov. 2017.
[15] W. Liu, "Optimal estimation for discrete-time linear systems in the presence of multiplicative and time-correlated additive measurement noises," *IEEE Trans. Signal Process.*, vol. 63, no. 17, pp. 4583–4593, Sep. 2015.
[16] Z. Gao, "Fractional-order Kalman filters for continuous-time linear and nonlinear fractional-order systems using Tustin generating function," *Int. J. Control*, vol. 92, no. 5, pp. 960–974, May 2019.
[17] Y. H. Sun, Y. Wang, X. P. Wu, and Y. L. Hu, "Robust extended fractional Kalman filter for nonlinear fractional system with missing measurement," *J. Franklin Inst.*, vol. 355, no. 1, pp. 361–380, 2018.
[18] D. Sierociuk and A. D. Nski, "Fractional Kalman filter algorithm for the states, parameters and order of fractional system estimation," *Int. J. Appl. Math. Comput. Sci.*, vol. 16, no. 1, 129–140, 2006.
[19] M. Xiao, Y. Zhang, Z. Wang, and H. Fu, "An adaptive three-stage extended Kalman filter for nonlinear discrete-time system in presence of unknown inputs," *ISA Trans.*, vol. 75, pp. 101–117, Apr. 2018.
[20] X. P. Wu, Y. H. Sun, Z. G. Lu, Z. N. Wei, and M. Ni, "A modified Kalman filter algorithm for fractional system under Lévy noises," *J. Franklin Inst.*, vol. 352, no. 5, pp. 1963–1978, 2015.
[21] Y. H. Sun, X. P. Wu, J. D. Cao, Z. N. Wei, and G. Q. Sun, "Fractional extended Kalman filtering for nonlinear fractional systems with Lévy noise," *IET Control Theory Appl.*, vol. 11, no. 3, pp. 349–358, 2017.
[22] Z. Gao, "Kalman Filters for continuous-time fractional-order systems involving fractional-order colored noises using Tustin generating function," *Int. J. Control Autom. Syst.*, vol. 16, no. 3, pp. 1049–1059, Jun. 2018.
[23] Z. Gao, "Cubature Kalman filters for nonlinear continuous-time fractional-order systems with uncorrelated and correlated noises," *Nonlinear Dyn.*, vol. 96, no. 3, pp. 1805–1817, May 2019.
[24] X. M. Huang, Z. Gao, R. C. Ma, and X. J. Chen, "Extended Kalman filters for fractional-order nonlinear continuous-time systems containing unknown parameters with correlated colored noises," *Int. J. Robust Nonlinear Control*, vol. 29, no. 17, pp. 5930–5956, 2019.
[25] B. Safarinejadian, N. Kianpour, and M. Asad, "State estimation in fractional-order systems with coloured measurement," *Trans. Inst. Meas. Control*, vol. 40, no. 6, pp. 1819–1835, 2018.
[26] F. Ding, *Modern Control Theory*. Beijing, China: Tsinghua Univ. Press, 2018.
[27] F. Ding, "System identification," in *New Theory and Methods*. Beijing, China: Science Press, 2013.
[28] C. Yang, Z. Gao, and F. H. Liu, "Kalman filter for linear continuous-time fractional-order systems involving coloured noises using fractional-order average derivative," *IET Control Theory Appl.*, vol. 12, no. 4, pp. 456–465, 2018.
[29] X. Zhang, C. Z. Wei, Y. M. Liu, and M. K. Luo, "Fractional corresponding operator in quantum mechanics and applications: A uniform fractional Schrodinger equation in form and fractional quantization methods," *Ann. Phys.*, vol. 350, pp. 124–136, 2014.
[30] B. M. Vinagre, Y. Q. Chen, and I. Petras, "Two direct Tustin discretization methods for fractional-order differentiator/integrator," *J. Rranklin Inst.-Eng. Appl. Math.*, vol. 340, no. 5, pp. 349–362, 2003.
[31] C. Scherer and S. Weiland, *Lecture Notes DISC Course on Linear Matrix Inequalities in Control* vol. 2, no. 1. Berlin, Germany: Springer-Verlag, 1999, pp. 69–70.

XIAOMIN HUANG received the B.S. degree in mathematics and applied mathematics (teacher-training) from Bohai University, Jinzhou, China, in 2017. She is currently pursuing the master's degree in operational research and cybernetics with Liaoning University, Shenyang, China. Her research interests include state estimation and parameter identification of fractional-order systems.

ZHE GAO received the Ph.D. degree in control theory and control engineering from the Beijing Institute of Technology, in 2012. He is currently an Associate Professor with the Department of Electrical Engineering and Automation, College of Light Industry, Liaoning University, China. He is also a master's student supervisor with the School of Mathematics, Liaoning University, China. He is doing Postdoctoral Research with Jilin University, China. His research interests include control, state estimation, and identification of fractional-order systems.

CHAO YANG received the B.S. degree in mathematics and applied mathematics from Shanxi Datong University, Datong, China, in 2016, and the M.S. degree in operational research and cybernetics from Liaoning University, Shenyang, China, in 2019. Her research interest includes the state estimation of fractional-order systems.

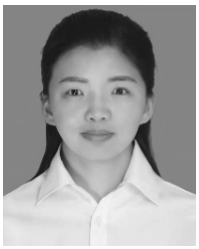

FANGHUI LIU received the B.S. degree from the School of Mathematics and System Science, Shandong Normal University, Jinan, China, in 2016, and the M.S. degree in operational research and cybernetics from Liaoning University, Shenyang, China, in 2019. Her research interests include fractional-order systems, state estimation, and Kalman filter.